
**MAGNETISM
AND FERROELECTRICITY**

Structural Self-Organization and the Formation of Perpendicular Magnetic Anisotropy in $\text{Co}_{50}\text{Pd}_{50}$ Nanocrystalline Films

L. I. Kveglis, S. M. Jarkov, and I. V. Staroverova

Kirensky Institute of Physics, Siberian Division, Russian Academy of Sciences, Akademgorodok, Krasnoyarsk, 660036 Russia

e-mail: jarkov@iph.krasnoyarsk.su

Received December 4, 2000

Abstract—The correlation of the atomic-order structure and the energy density of perpendicular magnetic anisotropy in $\text{Co}_{50}\text{Pd}_{50}$ films is investigated. Structural models for nanocrystalline $\text{Co}_{50}\text{Pd}_{50}$ films are proposed. It is shown that processes of structural self-organization in the films form nontrivial atomic-order structures. These structures can exist owing to high elastic stresses, which apparently ensure the emergence of strong magnetic anisotropy ($K_{\perp} \sim 10^6$ erg/cm³). © 2001 MAIK “Nauka/Interperiodica”.

1. INTRODUCTION

The existence of strong magnetic anisotropy perpendicular to the plane of a structurally disordered film has been studied by many authors engaged in research involving amorphous and nanocrystalline films. The strong dependence of the perpendicular magnetic anisotropy (PMA) constant on the technological conditions of preparation and processing of samples complicates unambiguous interpretation of the PMA origin. The possible mechanisms of PMA formation, which were analyzed comprehensively in [1], are determined by the atomic-order structure and chemical composition of the film. The main reasons behind the emergence of PMA in films are crystallographic anisotropy, anisotropy of the columnar structure, magnetostriction anisotropy, anisotropy of the local atomic ordering, surface anisotropy, and exchange anisotropy between multilayers (in the case of multilayered films). Connection of the columnar and fractal structures formed perpendicularly to the film plane with PMA exceeding the shape anisotropy of the film is visually demonstrated in [2–4]. However, the mechanisms and kinetics of formation of such structures remain unclear. In our previous publications [5–8], we proved that a local atomic order is formed in nanocrystalline films of transition metal alloys ($\text{Dy}_{23}\text{Co}_{77}$, $\text{Co}_{10}\text{Pd}_{90}$, and $\text{Co}_{50}\text{Pd}_{50}$) during preparation. We proposed that, in the case of Dy–Co alloys, PMA carriers are highly anisotropic clusters of the DyCo_5 type [6], while such carriers for Co–Pd alloys are clusters of the $L1_0$ and ϵ' phases, which are oriented so that the easy magnetization axis is perpendicular to the plane of the film [7, 8]. However, these phases were not always observed in the Co–Pd films. In some cases, PMA also took place without these phases [7] and the observed structure did not correspond to the phase equilibrium diagram.

Considerable deviations from equilibrium during the preparation of nanocrystalline materials lead to the formation of atomic structures that often do not conform to the equilibrium bulk state or to known metastable states of the given material. Away from the equilibrium state, an insignificant variation of the system parameter can result in a radical change in the physical properties of the substance [9]. The number and structure of defects in a nanocrystalline material differ qualitatively from those in mono- and polycrystalline materials; for this reason, the nanocrystalline state cannot be regarded simply as a monocrystalline state with a large number of defects [10]. Thus, the atomic structure of nanoparticles can be described in the framework of classical crystallography only for certain cases. The description of the atomic structure of the nanocrystalline state requires the application of nontraditional approaches.

One of such approaches is the Voronoï–Delone method developed for noncrystalline materials [11]. This method involves simulation of spatial structures with the help of Voronoï polyhedra. A Voronoï polyhedron is the direct geometrical image of the nearest atomic surrounding. The special significance of Voronoï polyhedra is that they are convenient structural elements for use in studying spatial structural motifs.

The above idea was developed further by Bulienkov *et al.* [12–14], who described the atomic structure of materials with amorphous, nanocrystalline, and quasi-crystalline discontinuous structures as an aggregate of crystalline modules. This concept is introduced in order to explain the mechanisms of self-organization of crystals and other structures with short-range and long-range order. This connects the energy of interatomic interaction and the geometry of the structure formation both on local and global levels. A crystalline module as

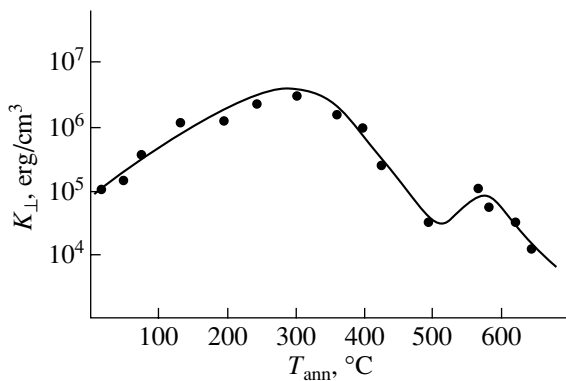


Fig. 1. Dependence of the perpendicular magnetic anisotropy constant K_{\perp} of a $\text{Co}_{50}\text{Pd}_{50}$ film on the annealing temperature T_{ann} .

a closed three-dimensional loop is repeated periodically in space and either fills the space entirely or embraces all the atoms of the structure through its apices, depending on the crystal symmetry. For example, a module of a face-centered cubic (fcc) lattice has the form of a primitive cell with fcc structure (in the form of a rhombohedron) and consists of an octahedron and two tetrahedra. Such an approach considerably extends the set of module polyhedra forming an atomically ordered structure as compared to the Fedorov groups and provides new opportunities to explain the unique physical properties of nanocrystalline materials.

The experiments on electron diffraction carried out by us earlier on Dy–Co and Co–Pd films [5–8] and the evolution of the concepts concerning the formation of the atomic structure in a structurally disordered material [11–14] led to the formulation of the following problems.

(1) The construction of structural models of short-range atomic ordering using the approaches described in [11–14] from an analysis of the electron diffraction patterns obtained for $\text{Co}_{50}\text{Pd}_{50}$ films with high PMA ($K_{\perp} \sim 10^6$ erg/cm³).

(2) The revision of the reasons behind the formation of PMA in the $\text{Co}_{50}\text{Pd}_{50}$ films under investigation on the basis of these structural models.

2. SAMPLE PREPARATION AND EXPERIMENTAL TECHNIQUE

In this work, we present the results of an investigation of the structure and magnetic properties of Co–Pd nanocrystalline films with equiatomic composition (50 at. % Co and 50 at. % Pd) in the initial state, as well as those subjected to thermal treatment in vacuum. The films were obtained by thermal sputtering–explosion in a vacuum of 10^{-5} Torr and through magnetron sputtering in a vacuum of 10^{-6} Torr on various substrates (glass, crystalline and amorphous silicon, fused quartz, NaCl, MgO, and LiF). The microscopic structure and

the phase composition of the films were studied using PREM-200 and JEM-100C transmission electron microscopes. The chemical composition of the films was monitored using x-ray fluorescence analysis. The PMA constant K_{\perp} was determined by the torque method at room temperature in fields of strengths up to 17 kOe.

3. RESULTS

The PMA constant of the films in the initial state was $K_{\perp} \sim 10^5$ erg/cm³ (Fig. 1). Electron diffraction patterns obtained from these films were in the form of a diffuse halo. Electron microscopic studies revealed that the films are composed of particles ≈ 20 – 30 Å in size. It was found that dendrite crystallization occurred in the films under the action of an electron beam in a transmission electron microscope or during annealing in a vacuum of 10^{-5} Torr at temperature $T_{\text{ann}} = 260$ – 300 °C. Figure 2a shows an electron microscope image of a region of dendrite grown in a nanocrystalline film. The velocity of the crystallization front determined visually from the electron-microscopic studies was up to 1 cm/s. After the completion of dendrite crystallization, no coarsening of the size of particles constituting the film was observed (as compared to the initial state). Figure 2b shows a magnified fragment of the pattern presented in Fig. 2a with the interface between the initial nanocrystalline phase (on the right) producing a diffuse halo on the electron diffraction pattern and the newly formed crystalline phase (on the left). An electron diffraction pattern of this region is given in Fig. 2c. The electron microscope image (Fig. 2b) demonstrates clearly that the film consists of particles of the same size. The electron diffraction pattern (Fig. 2c) obtained from crystallized regions (Figs. 2a, 2b) has a set of reflection points which do not correspond to any known structures of Co–Pd alloys. According to its phase equilibrium diagram, a Co–Pd alloy crystallizes into an fcc lattice with parameter $a = 3.75$ Å [15].

The electron diffraction pattern (Fig. 2c) clearly demonstrates considerable radial blurring for diffraction reflections at small angles, while groups of reflection points are observed instead of a single reflection at large angles. Such a pattern is not typical of film-type single crystals and indicates that, in this case, the film consists of microcrystallites coherently oriented relative to one another. The diffraction reflections observed on the electron diffraction pattern (Fig. 2c) correspond to the interplanar distances for atomic planes of the (111) and (620) types in the fcc structure with the lattice parameter $a = 3.75$ Å. Such a set of reflections can be observed on an electron diffraction pattern for the fcc lattice orientation with the [134] zone axis. However, in Fig. 2c, there are two extra reflections of the (111) type, as well as superstructure reflections for an fcc lattice, such as a group of reflections of the $(3/2 \ 1/2 \ 0)$, (310), and $(9/2 \ 3/2 \ 0)$ types. The intensities of these

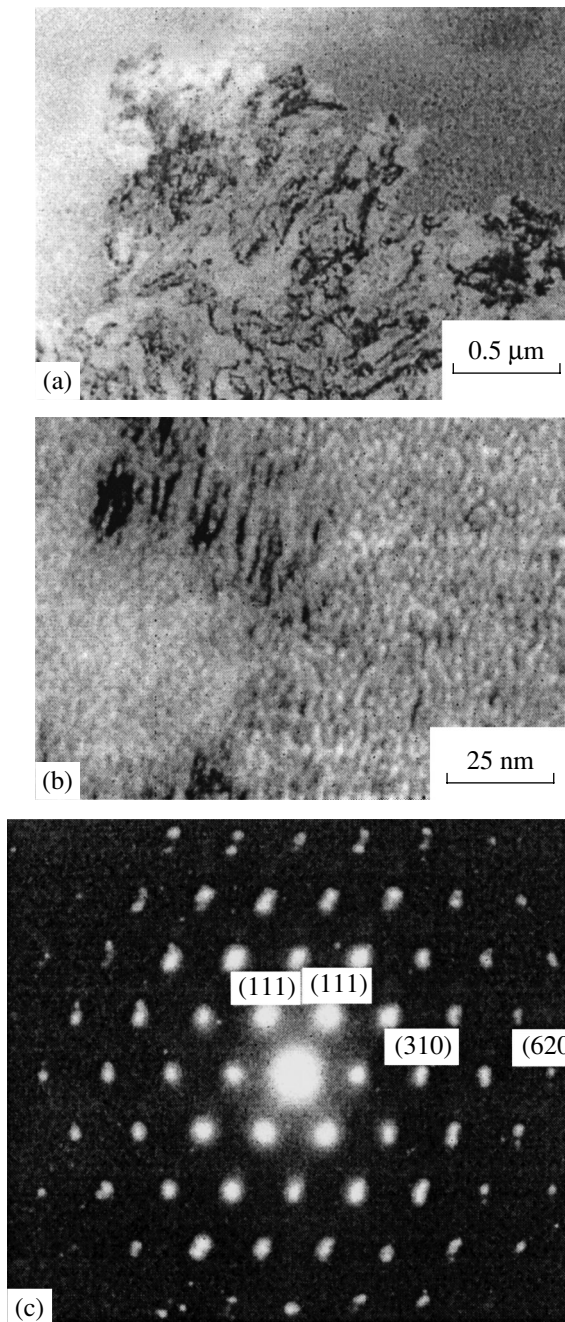


Fig. 2. (a, b) Electron microscope images of the crystallization front in a structurally disordered $\text{Co}_{50}\text{Pd}_{50}$ film after annealing ($T_{\text{ann}} = 260^\circ\text{C}$) with various magnifications and (c) the electron microdiffraction pattern from a crystallized region of the film.

superstructure reflections are much higher than the intensity of a structure reflection of the (620) type. It should be emphasized that on the electron diffraction pattern (Fig. 3a), the angle between vectors of the [111] and [310] types is $\approx 60^\circ\text{--}64^\circ$, whereas this angle must be equal to 68.58° in a cubic lattice.

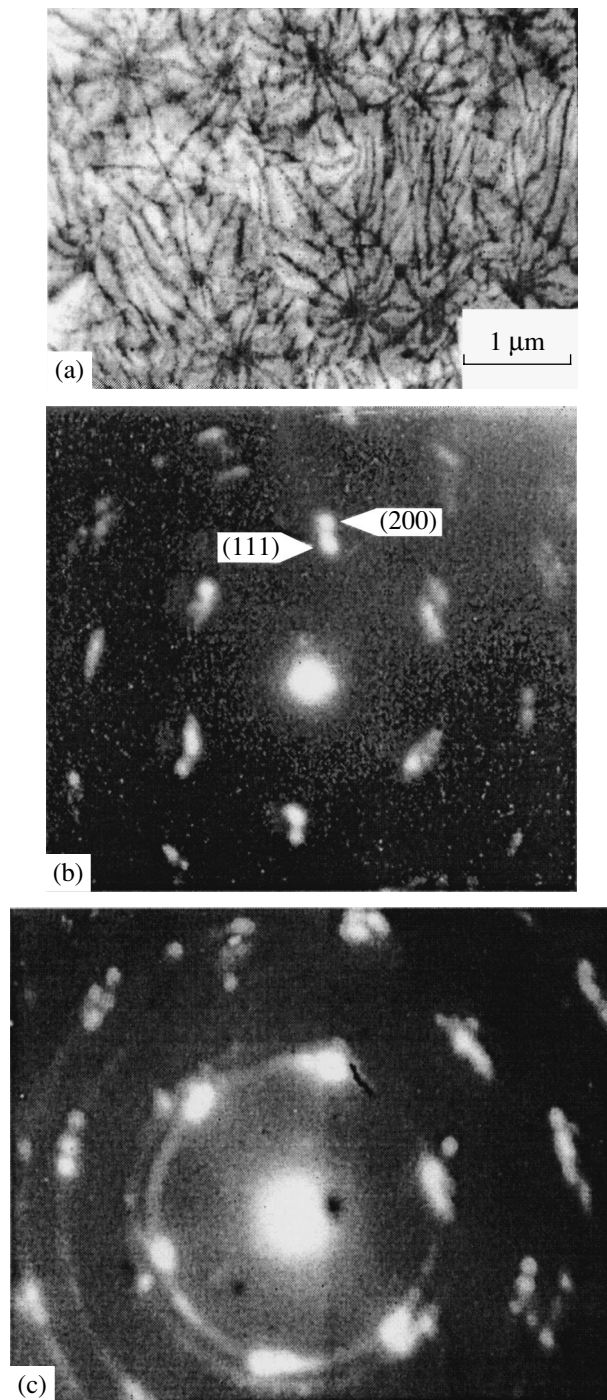


Fig. 3. (a) The electron microscope image with flexural loops and (b, c) electron microdiffraction patterns obtained from various regions of the $\text{Co}_{50}\text{Pd}_{50}$ film after annealing at $T_{\text{ann}} = 320^\circ\text{C}$.

After annealing at $T_{\text{ann}} > 300^\circ\text{C}$, the dendrite structure in the films began to disintegrate. An electron microscope image obtained for such a film is a continuous network of intersecting flexural extinction loops (Fig. 3a). An electron diffraction pattern obtained for a disintegrating dendrite is presented in Fig. 3b. This pat-

tern is also not typical. There are groups of reflections corresponding to the atomic (111) and (200) planes of the fcc structure ($a = 3.75 \text{ \AA}$) according to the interplanar distances. In this case, the [111] and [200] vectors are almost parallel to each other, which is impossible in principle for a single cubic crystal. It should be noted that the electron diffraction pattern presented in Fig. 3b was obtained by the method of microdiffraction from a region $\approx 0.5 \mu\text{m}$ in diameter. Such a pattern is typical of the films under study, but a film as a whole is not a single coherently oriented ensemble forming an electron diffraction pattern with regular reflection points. Electron diffraction patterns obtained from other regions of the film can have the form of a disordered set of reflection points. Moreover, for the same sample, there exist regions in which a structure of the type presented in Fig. 3b begins to be rearranged into a polycrystalline fcc structure (Fig. 3c).

Further annealing ($T_{\text{ann}} = 500^\circ\text{C}$) leads to the formation of atomically ordered phases typical of Co–Pd alloys [8, 16]: the $L1_0$ phase with a tetragonal face centered lattice and the ϵ' phase with a hexagonal close-packed (hcp) lattice. A distinguishing feature of all electron diffraction patterns obtained was that diffraction reflections from the $L1_0$ and ϵ' phases were always observed simultaneously and were oriented coherently with one another [7, 8]. After annealing at $T_{\text{ann}} \geq 650^\circ\text{C}$, the films displayed only equilibrium polycrystalline fcc structures ($a = 3.75 \text{ \AA}$).

The PMA constant K_{\perp} (Fig. 1) increased during annealing to $6 \times 10^6 \text{ erg/cm}^3$ as a result of the formation of the dendrite structure ($T_{\text{ann}} = 260\text{--}300^\circ\text{C}$) and then decreased to $5 \times (10^5\text{--}10^4) \text{ erg/cm}^3$ upon disintegration of this structure ($T_{\text{ann}} = 300\text{--}500^\circ\text{C}$). After the formation of the atomically ordered $L1_0$ and ϵ' phases ($T_{\text{ann}} = 560^\circ\text{C}$), the value of K_{\perp} increased to 10^5 erg/cm^3 . Further annealing ($T_{\text{ann}} = 560^\circ\text{C}$) led to the formation of a polycrystalline fcc structure and a monotonic decrease in the value of the PMA constant. Our investigations did not reveal any fundamental difference in the atomic structure and magnetic properties for $\text{Co}_{50}\text{Pd}_{50}$ films obtained by different methods on different substrates.

4. DISCUSSION

As was mentioned above, the electron diffraction patterns obtained from $\text{Co}_{50}\text{Pd}_{50}$ films after dendrite crystallization did not correspond to any of the known phases of Co–Pd alloys. Attempts to interpret the electron diffraction pattern in Fig. 2c from the viewpoint of densely packed structures proved to be futile. For instance, the electron diffraction pattern from an hcp structure with the $[01\bar{1}1]$ zone axis resembles that in Fig. 2c. However, in order to form such an electron diffraction pattern, an hcp lattice with parameters $a = 2.69 \text{ \AA}$ and $c = 5.87 \text{ \AA}$ would be required. First, such a structure is unknown for Co–Pd alloys and, second,

many high-intensity reflections observed on the electron diffraction pattern in Fig. 2c (e.g., $[\bar{1}\bar{1}21]$, $[2\bar{1}\bar{1}1]$) correspond to a superstructure for an hcp lattice. In this case, special attention should be paid to the value of the ratio (c/a) ≈ 2.18 . It is well known that metals form close-packed crystalline structures; i.e., the ratio c/a for an hcp lattice in the ideal case must be equal to 1.633. Crystallization in the films under investigation occurs at high rates. For this reason, the electron diffraction pattern depicted in Fig. 2c cannot be attributed to atomic ordering, since the time is obviously insufficient for ordering to occur. A possible explanation of the formation of electron diffraction patterns that are not typical of Co–Pd alloys is the formation of intermetallic compounds. However, this assumption is also groundless since, first, the diffraction reflections corresponding to large interplanar distances that are necessarily observed for intermetallides are absent on the electron diffraction patterns and, second, the formation of intermetallides requires a large amount of impurities, while the concentration of impurities in the films obtained by magnetron sputtering in a vacuum of 10^{-6} Torr does not exceed 1 at. %. The films obtained by the method of thermal sputtering–explosion cannot also contain a large amount of impurities. Attempts to explain the observed electron diffraction patterns using the effect of twinning of known structures did not lead to positive results either. All that has been said above also respectively refers to the electron diffraction pattern presented in Fig. 3b. We considered another possibility for the formation of the electron diffraction pattern in Fig. 3b on the basis of coherent mutual orientation of microcrystallites with different orientations relative to the substrate (i.e., through superposition of the electron diffraction patterns obtained for different orientations). It was found that this electron diffraction pattern cannot be formed in this way.

In order to explain the formation of the atomic order and to interpret the electron diffraction patterns obtained from the films under investigation, we proceeded from the assumptions developed in [11–14]. However, in contrast to those publications, we employed, instead of Voronoï polyhedra or Bulienkov crystalline modules, assemblies of modules consisting of octahedra and tetrahedra, which can be used for describing close-packed structures of metals. A common feature between our approach with the Voronoï–Delone methods and the Bulienkov method is that the module assemblies fill the space through percolation rather than through translations.

Here, we propose schemes of module assemblies that help to explain the formation of the electron diffraction patterns (Figs. 2c, 3b) obtained from $\text{Co}_{50}\text{Pd}_{50}$ films. Figures 4a and 4b show module assemblies that help to explain the formation of the electron diffraction patterns in Figs. 2c and 3b. The modules are connected

through common faces, where the atoms are located at the sites. The indices on the vectors in Figs. 4a and 4b denote the serial numbers of such modules. Such assemblies can be repeated in space in various ways, e.g., in the form of a Boerdijk spiral [11, 17] supplemented with octahedra by analogy with the intergrowth rods described in [13]. These assemblies can rearrange themselves from the hcp to the fcc structure. The proposed module assemblies help to explain the possible formation of planar atomic networks in dendritic structures, which create conditions for electron diffraction and the emergence of diffraction reflection points on electron diffraction patterns. Such planar atomic networks with a high local density of atoms are responsible for the emergence of high-intensity superstructure reflections on the electron diffraction patterns. The module assemblies proposed by us also help to explain the formation of nonstandard angles on the electron diffraction patterns. The filling of 3D space with module assemblies occurs through their fitting with one another through common faces. As a result, a fractal (dendrite) structure is formed in which all vectors genetically present in the module assembly are preserved. The structures formed from such assemblies (see Figs. 4a, 4b) can obviously be regarded as quasi-crystalline. In such a structure, atoms are arranged in a quasi-periodic sequence. In spite of the fact that such a structure does not possess translational symmetry, a system of reflection points is formed on the electron diffraction pattern for a certain orientation of this structure [18, 19].

The formation of the electron diffraction pattern presented in Fig. 2c can be explained by a scheme of module assembly consisting of three modules (see Fig. 4a). Each module, in turn, is formed by a tetrahedron and an octahedron. The assembly is organized so that three tetrahedra are connected through common faces. In Fig. 4a, the tetrahedron of the second module is indicated by dashed lines and is behind the plane of the figure. The $[111]$ vectors do not lie in the plane of the figure, and the scheme shows the projections of these vectors. The $[310]$ vectors of the first and third modules have a common point and are almost antiparallel. The disorientation angle amounts to $\approx 4.5^\circ$ and is manifested on the electron diffraction pattern in Fig. 2c in the form of a splitting of the (310)-type reflections. The angle formed by the $[111]$ vectors of the first and third modules in the assembly is $\approx 56^\circ$; this angle is observed in the experimental electron diffraction pattern (Fig. 2c).

Figure 4b shows a scheme that enables us to interpret the electron diffraction pattern in Fig. 3b obtained from a dendrite undergoing destruction. The scheme is a system of three fcc modules (denoted by Roman numerals in the figure) supplemented with tetrahedra. The (110) planes of the modules coincide with the plane of the figure. The (111) plane of the tetrahedron at the center of the system also coincides with the plane of the figure. This tetrahedron is connected with each fcc module through another tetrahedron. According to this scheme, the $[111]$ vector of the first module in such

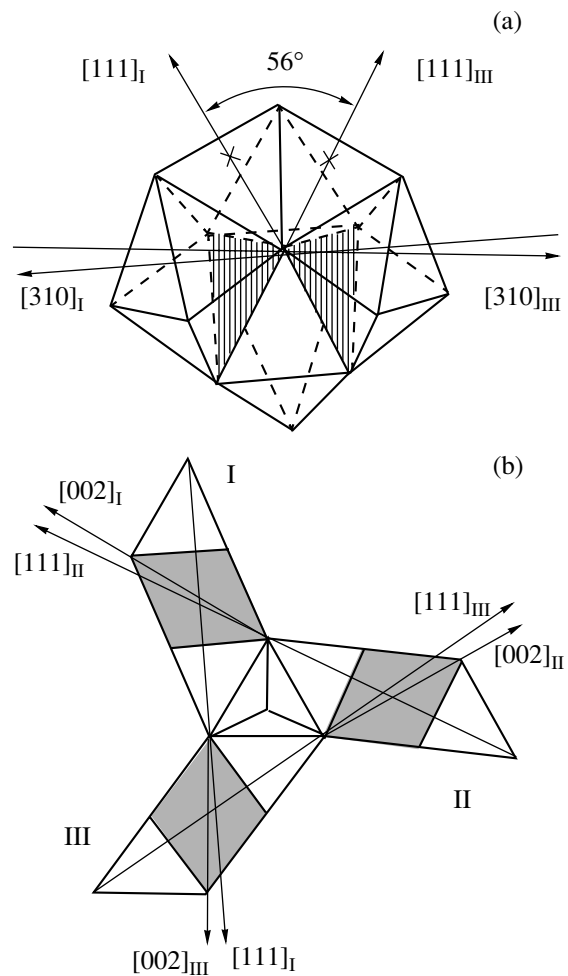


Fig. 4. (a, b) Diagrams of module assemblies explaining the formation of the electron diffraction patterns presented in Figs. 2c and 3b, respectively. The indices correspond to the fcc structure.

a module assembly is almost parallel to the $[002]$ vector of the third module, the mismatching angle between the vectors being $\approx 5.3^\circ$. This explains the disorientation of vectors of the $[111]$ and $[200]$ types that is observed in the electron diffraction pattern in Fig. 3b.

An analysis of the dendrite crystallization rate in our films and of the observed morphological instabilities of the crystallization front and the fact that dendrite crystallization does not result in an increase in the size of particles constituting the film as compared to the initial state lead one to the conclusion that the crystallization in the investigated films is a diffusionless (i.e., kinetic) process. As a rule, such a crystallization is explosive and is accompanied by the formation of a liquid zone (having a size of ~ 20 Å) at the crystallization front [20]. The velocity of this front is so high that nanoparticles go over to a liquidlike state (so-called virtual melting [21] or quasi-melting [22]). The liquid interlayer ensures the conditions for the fitting of nanoparticles with one another. The morphology of dendrites formed

in this case is determined by the internal structure of nanoparticles. Their structure, in turn, is a result of module self-organization, which is reduced to a combination of module assemblies through common faces. In this case, nonideal filling of space takes place. The mismatching angle between the faces of adjacent module assemblies can be as large as several degrees. As a result, considerable stresses appear in the material. These stresses are partly removed by the displacements of atomic complexes, discontinuities, and cracks. The presence of internal stresses in the films under investigation is confirmed by the observation of tension bars in electron diffraction patterns and flexural loops in electron microscope images (Fig. 3a). Considering that Co–Pd alloys have a high magnetostriction, we can assume that magnetostriction makes a significant contribution to the formation of large values of the PMA constant in the initial state, as well as in the presence of a dendrite structure. The destruction of the dendrite quasi-crystalline structure leads to the formation of atomically ordered highly anisotropic $L1_0$ and ϵ' phases. The coherent orientation of these phases is ensured by the common elements of the structure (tetrahedra and octahedra). The value of the PMA constant in this case is determined by the crystallographic anisotropy of the $L1_0$ and ϵ' phases.

Thus, the interpretation of the electron diffraction patterns and the analysis of the peculiarities in the growth of dendrite structures in nanocrystalline $\text{Co}_{50}\text{Pd}_{50}$ films allowed us to construct a model of the nearest atomic surrounding in $\text{Co}_{50}\text{Pd}_{50}$ films with a high value of the PMA constant. It is shown that the main contribution to the magnetic anisotropy perpendicular to the film surface comes from the effects associated with the structural organization of crystalline modules.

ACKNOWLEDGMENTS

The authors are grateful to V.N. Matveev for providing the samples obtained using magnetron sputtering, to G.V. Bondarenko for analyzing the chemical composition of the films using the x-ray fluorescence method, and to N.A. Bulienkov, V.A. Petrov, and V.C. Gouliaev for useful discussions and valuable remarks.

This work was supported by the Russian Foundation for Basic Research (project no. 00-02-17358a), and by the Krasnoyarsk Krai Science Foundation.

REFERENCES

1. W. H. Meiklejohn, Proc. IEEE **74** (11), 1570 (1986).
2. H. J. Leamy and A. G. Dirks, J. Appl. Phys. **49** (6), 3430 (1978).
3. H. J. Leamy and A. G. Dirks, J. Appl. Phys. **50** (4), 2871 (1979).
4. T. Suzuki, Jpn. J. Appl. Phys. **23** (5), 585 (1984).
5. L. I. Vershinina-Kveglis, V. S. Zhigalov, A. V. Zhuravlev, and G. I. Frolov, Fiz. Met. Metalloved., No. 4, 62 (1991).
6. A. S. Avilov, L. I. Vershinina-Kveglis, S. V. Orekhov, *et al.*, Izv. Akad. Nauk SSSR, Ser. Fiz. **55** (8), 1609 (1991).
7. L. I. Vershinina-Kveglis, V. A. Petrov, and T. G. Popova, Fiz. Met. Metalloved. **58** (5), 980 (1984).
8. L. I. Vershinina-Kveglis, V. S. Zhigalov, I. V. Staroverova, *et al.*, Fiz. Tverd. Tela (Leningrad) **33** (5), 1409 (1991) [Sov. Phys. Solid State **33**, 793 (1991)].
9. I. Prigogine, *The End of Certainty. Time, Chaos and the New Laws of Nature* (The Free Press, New York, 1997).
10. H. Gleiter, Acta Mater. **48** (1), 1 (2000).
11. N. N. Medvedev, *Voronoi–Delone Method in Research of Noncrystalline Systems Structure* (Novosibirsk, 2000).
12. N. A. Bulienkov, Vestn. Nizhegor. Univ., Ser. Fiz. Tverd. Tela **1**, 19 (1998).
13. N. A. Bulienkov and V. S. Kraposhin, Pis'ma Zh. Tekh. Fiz. **19** (23), 1 (1993) [Tech. Phys. Lett. **19**, 739 (1993)].
14. P. V. An and N. A. Bulienkov, Mater. Sci. Res. **6** (1), 22 (2000).
15. R. M. Bozorth, *Ferromagnetism* (Van Nostrand, New York, 1951; Inostrannaya Literatura, Moscow, 1956).
16. V. Matsuo, J. Phys. Soc. Jpn. **32** (4), 972 (1972).
17. A. H. Boerdijk, Philips Res. Rep. **7**, 303 (1952).
18. D. Levine and P. J. Steinhardt, Phys. Rev. Lett. **53** (26), 2477 (1984).
19. G. M. Zaslavskii, R. Z. Sagdeev, D. A. Usikov, and A. A. Chernikov, Usp. Fiz. Nauk **156** (2), 193 (1988) [Sov. Phys. Usp. **31**, 887 (1988)].
20. V. A. Shklovskii and V. M. Kuz'menko, Usp. Fiz. Nauk **157** (2), 311 (1989) [Sov. Phys. Usp. **32**, 163 (1989)].
21. V. S. Ivanova, A. S. Balankin, I. Zh. Bunin, and A. A. Oksogoev, *Synergetics and Fractals in Material Science* (Nauka, Moscow, 1994).
22. P. M. Ajayan and L. D. Marks, Phys. Rev. Lett. **63** (3), 279 (1989).

Translated by N. Wadhwa